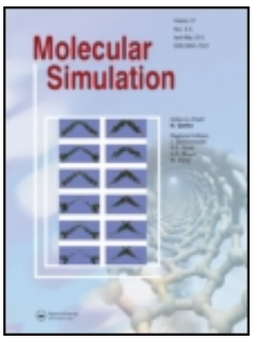

Molecular Simulation

ISSN: 0892-7022 (Print) 1029-0435 (Online) Journal homepage: https://www.tandfonline.com/loi/gmos20

Methane diffusion mechanism in catenated metal–organic frameworks

Chunyu Xue , Zie Zhou , Bei Liu , Qingyuan Yang & Chongli Zhong

To cite this article: Chunyu Xue , Zie Zhou , Bei Liu , Qingyuan Yang & Chongli Zhong (2009) Methane diffusion mechanism in catenated metal–organic frameworks, Molecular Simulation, 35:5, 373-380, DOI: 10.1080/08927020802609447

To link to this article: https://doi.org/10.1080/08927020802609447

Published online: 24 Mar 2009.

Molecular Simulation
Vol. 35, No. 5, April 2009, 373–380

Taylor & Francis
Taylor & Francis Group

Methane diffusion mechanism in catenated metal–organic frameworks

Chunyu Xue[a], Zie Zhou[a], Bei Liu[b], Qingyuan Yang[a] and Chongli Zhong[a]*

[a]*Laboratory of Computational Chemistry, Department of Chemical Engineering, Beijing University of Chemical Technology, Beijing, People's Republic of China;* [b]*Department of Chemical Engineering, University of California, Berkeley, USA*

(*Received 13 August 2008; final version received 6 November 2008*)

In this work, molecular dynamics simulations were performed to investigate the gas diffusion mechanism in catenated metal–organic frameworks (MOFs), for which methane was adopted as a probe and two catenated IRMOFs with interwoven structure, IRMOF-11 and IRMOF-13, were considered. This work reveals that the diffusion pathways of methane molecules in catenated MOFs are mainly governed by the strong confinement in catenation regions, leading to a 3D diffusion along the sheets formed by the A-regions (*xy*-direction) as well as from one A-region to another by crossing a B-region (*z*-direction). In addition, the present work shows that the effect of catenation on methane diffusivity is very large, much larger than that on hydrogen diffusivity at room temperature, and that both adsorption selectivity and dynamic selectivity of gas mixtures may be enhanced largely in catenated MOFs, indicating that catenation is a good strategy to improve the overall performance of a material as a membrane in separation applications.

Keywords: diffusion mechanism; catenated metal–organic framework; molecular dynamics

1. Introduction

Metal–organic frameworks (MOFs) are a class of new nanoporous materials that have emerged as promising for gas storage, separation and catalysis, etc. [1–3]. In many potential applications, knowledge of both gas adsorption and diffusion is important. Although extensive studies have been carried out on the adsorption behaviour of gases and gas mixtures in MOFs both experimentally [4–12] and theoretically [13–22], those on molecular diffusion in MOFs are far less since it is much more difficult to measure accurately the diffusivity of gas inside nanoporous materials by experiment. Thus, molecular simulation plays an important role in understanding molecular diffusion in this kind of material. To the best of our knowledge, there are only a couple of experimental studies to date on gas diffusion in MOFs [23–25], and most knowledge on this topic was obtained by molecular simulations [26–35]. For example, Skoulidas [26] and Skoulidas and Sholl [27] investigated the self- and transport diffusivity of several light gases in MOFs using the molecular dynamics (MD) method, Yang and Zhong [28] performed a molecular simulation study on the diffusion of hydrogen in several MOFs, while Keskin et al. [33] used molecular simulations to study diffusion of CH_4/H_2 mixtures in Cu-BTC and they also presented the information about the performance of MOF-5 as a membrane for separation of CO_2/CH_4 mixtures [34].

It is well known that additional pores with various sizes are generated by the catenation of frameworks, leading to catenated MOFs that exhibit enhanced gas adsorption [36–38] and separation performance [39–41]. However, little is known about the gas diffusion characteristics in such catenated MOFs. In our previous work [31], we showed that catenation can reduce hydrogen diffusivity by a factor of 2–3 at room temperature. However, in the case of hydrogen at room temperature, the effect of catenation on diffusion is mainly attributed to the steric hindrance since H_2 molecules are hardly adsorbed on MOFs at room temperature. Thus, in this work, we further studied the diffusion of methane in these materials, which allows us to investigate the effect of catenation on gas diffusion, where both adsorbate/adsorbent interactions and steric hindrance work. In addition, in our previous work, only the effect of catenation on the value of gas diffusivity was studied [31], while in this work we focused on the diffusion mechanism.

2. Models and computational method

2.1 MOF structures

Catenated MOFs have a somewhat more complicated structure, which has been found to show enhanced gas adsorption and separation performance. Therefore, this work focuses on the gas diffusion mechanism in this kind of MOFs. For this purpose, we adopted two interwoven IRMOFs, IRMOF-11 and IRMOF-13, as the representatives of catenated MOFs. To make a comparison, their corresponding non-interwoven counterparts, IRMOF-12 and IRMOF-14, were also considered. IRMOF-12 and IRMOF-14 have the same cubic topology with the

*Corresponding author. Email: hzhongcl@mail.buct.edu.cn

ISSN 0892-7022 print/ISSN 1029-0435 online

DOI: 10.1080/08927020802609447
http://www.informaworld.com

octahedral $Zn_4O(CO_2)$ clusters linked by different organic dicarboxylate linkers, while IRMOF-11 and IRMOF-13 are their corresponding interwoven counterparts. Details of their structures and properties can be found elsewhere [12].

2.2 *Force fields*

In the present work, methane molecules were modelled as a single Lennard-Jones (LJ) interaction site using the parameters obtained by Goodbody et al. [42]. For the atoms in the framework of MOF materials, the universal force field of Rappé et al. [43] was adopted. The potential parameters used in this work were listed in Table 1. All the LJ cross-interaction parameters were determined by the Lorentz–Berthelot mixing rules.

The above set of force fields has been successfully employed to depict alkane adsorption [19,22], separation [39,44,45] and diffusion [30] in MOFs by several groups. To further confirm the reliability of the above set of force fields adopted in this work, the adsorption isotherms of CH_4 in IRMOF-1 and IRMOF-6 were simulated and compared with the experimental data [12], as shown in Figure 1. The results show that the simulations give good agreement with experimental adsorption isotherms, and similar conclusion has also been obtained by Düren et al. [19]. This demonstrates that the set of force fields adopted in this work can give a reliable estimation of the methane adsorption in IRMOFs, and thus can be used to study methane diffusion in IRMOFs.

2.3 *Molecular dynamics simulation*

In this work, equilibrium MD simulation was used to investigate the effects of catenation on methane diffusion as well as the diffusion mechanism of methane in catenated IRMOFs. All the MD simulations were performed under room temperature, which was held constant with a Nose–Hoover chain thermostat as formulated by Martyna et al. [46]. Similar to previous works [26–34], all the IRMOFs were treated as rigid with atoms frozen at their crystallographic positions during simulations. The simulation cell consists of 2 × 2 × 2 to 4 × 4 × 4 elementary cells of the IRMOF crystal lattice to ensure at least 50 CH_4 molecules are accommodated in the cell. The velocity Verlet algorithm was used to integrate Newton's equations of motion. The time step used in the MD simulations was taken as 1.0 fs. All the LJ interactions were calculated using the cut and shifted potential with a 15.0 Å cut-off radius, and periodic boundary conditions were applied in all three dimensions. Each MD simulation started with the random insertion of the molecules into the IRMOF lattices, and then relaxed using approximately 100,000 NVT Monte Carlo moves followed by 500,000 MD steps. After equilibration, the simulations were run for 2,500,000 MD steps to sample the diffusion properties of interest. At least 10 independent simulations were performed for each loading to estimate the statistical error. During each simulation, the trajectory of the system was saved every 100 steps to calculate subsequently the self-diffusion coefficient D_s by mean-square displacements method. It was checked that MD simulations conducted in microcanonical (NVE) ensemble gave the equivalent results.

Table 1. LJ potential parameters for CH_4 and the IRMOFs used in this work.

LJ parameters	CH_4	MOF_O	MOF_C	MOF_H	MOF_Zn
σ (Å)	3.73	3.12	3.43	2.57	2.46
ε/k_B (K)	148.0	30.19	52.84	22.14	62.40

3. Results and discussion

3.1 *Effect of catenation on methane diffusivity in IRMOFs*

To understand the effect of catenation on methane diffusivity in IRMOFs, MD simulations were performed to calculate the self-diffusivities of CH_4 in the two pairs of IRMOFs at room temperature. The simulation results are shown in Figure 2(a), as a function of methane loading. The methane self-diffusivities in the IRMOFs without catenation (IRMOF-12 and IRMOF-14) are about three to five times higher than that in their corresponding catenated counterparts (IRMOF-11 and IRMOF-13), indicating that

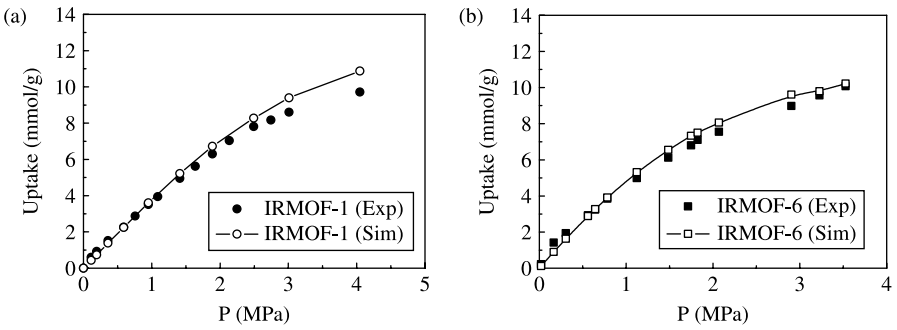

Figure 1. Experimental [12] and simulated methane adsorption isotherms at 298 K: (a) IRMOF-1 and (b) IRMOF-6.

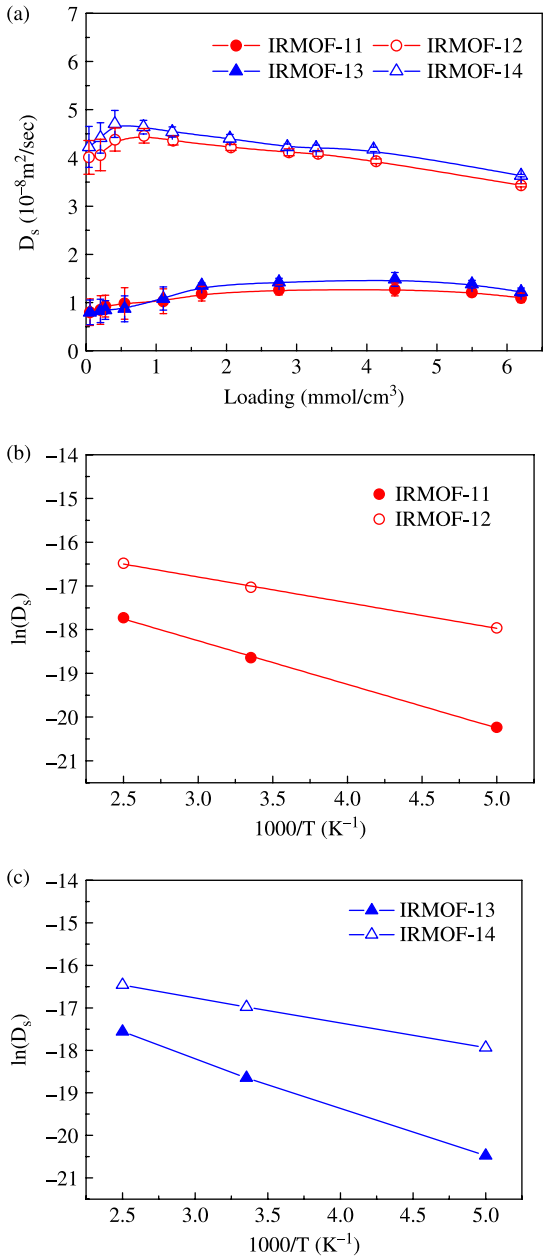

Figure 2. (a) Self-diffusivity of methane in the two pairs of IRMOFs at room temperature and (b,c) Arrhenius plots of *D*s for methane in the IRMOFs at infinite dilution at 200, 298 and 400 K.

the motion of methane molecules in catenated IRMOFs is restricted largely by their catenated structures. This phenomenon is consistent with the H_2 diffusion in these IRMOFs [31]; however, the effect of catenation on methane diffusivity is much larger than that on H_2 [31]. This observation may be explained as follows: the motion of both CH_4 and H_2 is restricted by the catenated structure, while the stronger interactions between CH_4 and the catenated framework lead to stronger confinement effects than that of H_2 in these catenated IRMOFs.

The self-diffusivity of methane increases slightly at first followed by a decrease with further increasing methane loading. This behaviour has also been observed elsewhere [26,28]. It can be explained as follows: at low loadings, CH_4 can diffuse mainly through the favourable adsorption sites leading to a high activation energy; at higher loadings, the pathway through the favourable adsorption sites is increasingly less favourable leading to a lower activation energy for diffusion, thus an increase in methane diffusivity; at even higher loadings, the concentration dependence arises as a natural consequence of steric hindrance between the diffusing molecules, resulting in a lowering of methane self-diffusivity.

Diffusion of CH_4 in IRMOFs was found to be an activated process, as in zeolites. The infinite-dilution activation energies for methane diffusion in the two pairs of IRMOFs shown in Figure 2(b) and (c) were calculated by performing MD simulations at three temperatures: $T = 200$, 300 and 400 K. The values obtained are 8.29 and 9.65 kJ/mol for IRMOF-11 and IRMOF-13, respectively, which are much larger than that in their corresponding non-catenated counterparts with the values of 4.89 and 4.90 kJ/mol for IRMOF-12 and IRMOF-14, respectively. The infinite-dilution activation energy of CH_4 in silicalite is found experimentally to be 5.7 kJ/mol [47] and the simulated result is 4.4 kJ/mol [48]. Therefore, the activation energy in the non-catenated IRMOFs is similar to that in silica zeolites, while it is greatly increased in its corresponding catenated IRMOFs, causing a much lower diffusivity in them.

3.2 Comparison of the effect of catenation on diffusivity of methane and hydrogen in IRMOFs

In practical applications, such as membrane-based separations, the relative diffusivity of molecules inside the materials plays an important role in determining the overall performance of a material. Figure 3 shows the loading dependency of relative diffusivity D_r of H_2 to CH_4

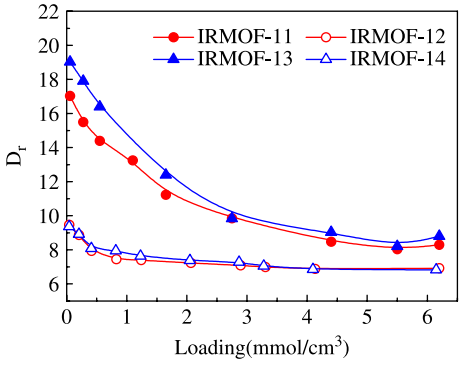

Figure 3. Comparison of the relative diffusivity of hydrogen to methane in the IRMOFs at room temperature.

at room temperature in the two pairs of IRMOFs, which is defined as $D_r = D_{H_2}/D_{CH_4}$. As can be seen from this figure, the relative diffusivity in the catenated IRMOFs is much higher than those in their corresponding non-catenated counterparts, indicating that catenation can significantly enhance the dynamic selectivity for CH_4/H_2 system, particularly at low loadings. This can be attributed to the much larger effect of catenation on methane diffusivity than that on hydrogen diffusivity.

Our previous work [39] has shown that the adsorption selectivity of CH_4/H_2 mixtures is greatly enhanced in catenated IRMOFs compared with their non-catenated counterparts. This work further demonstrated that the dynamic selectivity of this mixture can also be greatly enhanced in the catenated IRMOFs. Thus, catenation is a good strategy to improve the overall performance of a membrane material for separation applications. However, in this work we simply compared the diffusivity of pure components under same conditions, and a direct calculation of mixture diffusivity can give more insights, which is under studying in our group.

3.3 *Diffusion mechanism*

As the structures of catenated IRMOFs are somewhat more complicated, the diffusion mechanism is not clear to date. To understand more deeply the effect of catenation on molecule diffusion at the microscopic level, the diffusion mechanism at low loadings was further studied in detail. Because the structure of IRMOF-11 is similar to that of IRMOF-13, we only showed the diffusion mechanism of methane in IRMOF-13 as an example. The structural model was constructed from the XRD data given by Eddaoudi et al. [12], as shown in Figure 4. IRMOF-13 consists of two kinds of regions: those (labelled as A) formed by six pairs of metal clusters and face-to-face organic linkers (Figure 4(a)) and those (labelled as B) formed by six pairs of metal clusters and coplanar organic linkers (Figure 4(b)). The A-regions connect to each other (along the *xy*-direction) to form an A-sheet, which is also the case for B-regions (Figure 4(c)). Furthermore, the A- and B-sheets connect (along the *z*-direction) alternately to form the 3D material of IRMOF-13 (Figure 4(d)).

The centre of mass (COM) probability distributions of methane in the two kinds of sheets at two loadings were shown in Figures 5 and 6, in which Figure 5 was drawn to describe the COM probability distributions of methane in the A-sheet, while Figure 6 in the B-sheet. As can be seen from Figures 5 and 6, methane molecules mainly accumulate in the A-sheet at very low loading, while more molecules become to accumulate in the B-sheet at higher loading. Careful examination of the COM probability

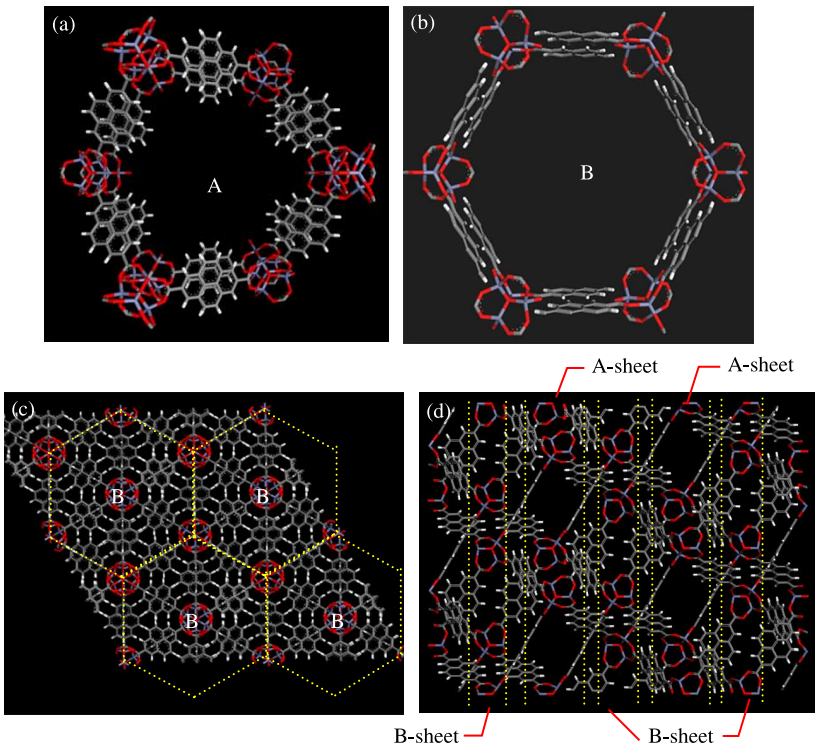

Figure 4. The crystal structure of IRMOF-13. (a) A-region formed by six pairs of metal clusters and face-to-face organic linkers, (b) B-region formed by six pairs of metal clusters and coplanar organic linkers, (c) super cell of IRMOF-13 consisting of 2 × 2 × 1 unit cells viewed from [0,0,1] and (d) super cell of IRMOF-13 consisting of 2 × 2 × 1 unit cells viewed from [1,0,0] (Zn, blue; O, red; C, grey and H, white).

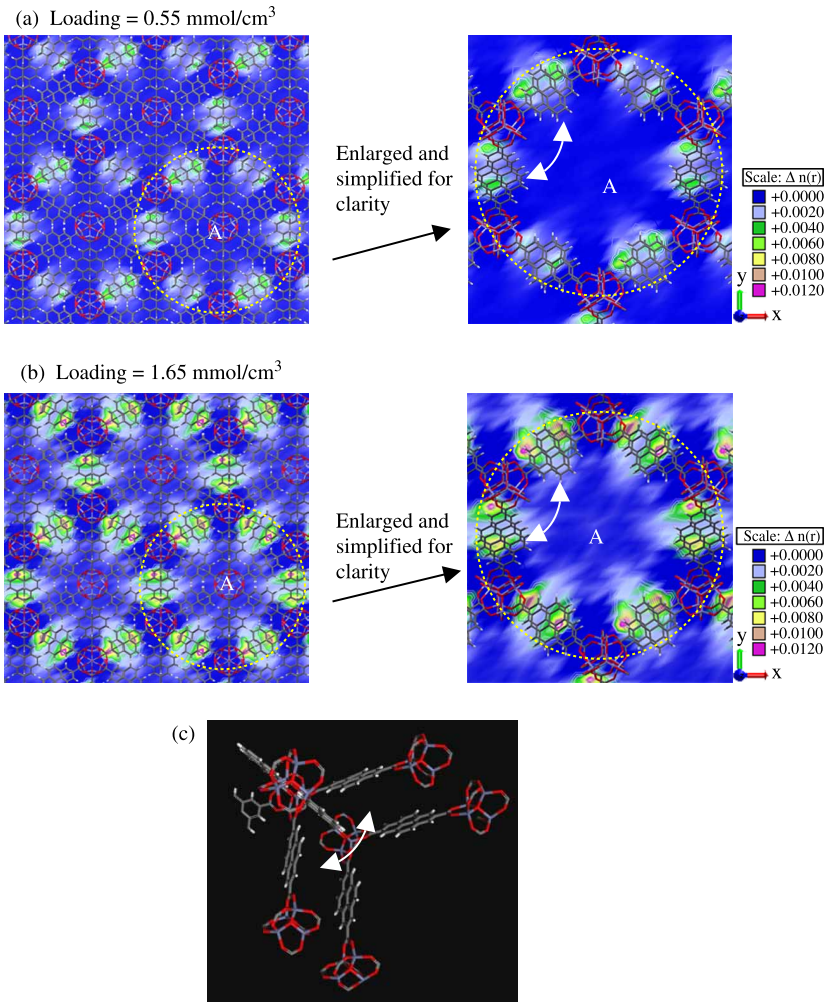

Figure 5. Contour plots of COM probability density of methane in the A-regions of IRMOF-13.

density led us to propose the following mechanism: methane diffusion in the *xy*-direction mainly occurs in the A-sheets as indicated in Figure 5(a) and (b), for which a methane molecule hops from one region formed by the face-to-face organic linkers to another across the top of the metal site indicated in Figure 5(c). As for the B-sheets, the methane diffusion is on the circled surface of B-regions (Figure 6), and the diffusion pathways between the B-regions are blocked in the *xy*-direction by the coplanar linkers. Thus, the main role of B-regions is as the passages between the A-sheets in the *z*-direction. Obviously, at very low loadings, methane diffusion mainly occurs in the A-sheets, while with increasing loading the diffusion passing B-regions becomes more evident. To understand the diffusion pathways between the A- and B-sheets, the COM probability density along the *z*-direction at several loadings was further examined, and the results at the loading of 1.65 mmol/cm^3 are shown in Figure 7(a) as an example. The most probable pathway in the *z*-direction is that a methane molecule hops from one A-sheet to another through one B-region (Figure 7(a)) by jumping through the surface of one linker between the A- and B-regions (Figure 7(b)). Based on the above discussions, it is clear that the diffusion of methane was mainly governed by the strong confinement in catenation regions, leading to a 3D diffusion along the sheets formed by A-regions (*xy*-direction) as well as from one A-region to another by crossing a B-region (*z*-direction).

Finally, it should be pointed out that in our simulations the frameworks are treated as rigid, while MOFs are vibrating at room temperature which might affect the diffusivity of methane to some extent. However, since the interactions between methane and the MOFs are not very strong and the temperature is not high, it is expected that the flexibility of the IRMOFs is not so serious to affect the diffusion mechanism of methane, and thus the mechanisms obtained with rigid framework should be the same with flexible framework. This can also be supported by the investigation of Amirjalayer et al. [35]. In their work, they studied the diffusivity and diffusion mechanism of several hydrocarbons in IRMOF-1 based on flexible framework;

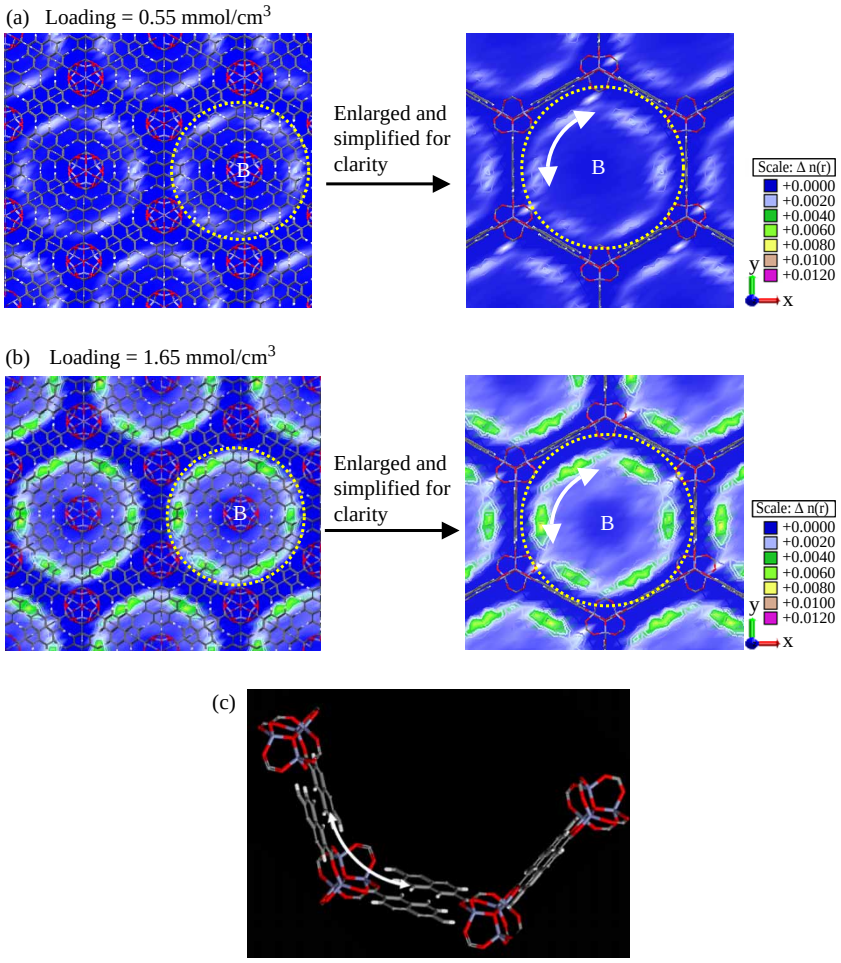

Figure 6. Contour plots of COM probability density of methane in the B-regions of IRMOF-13.

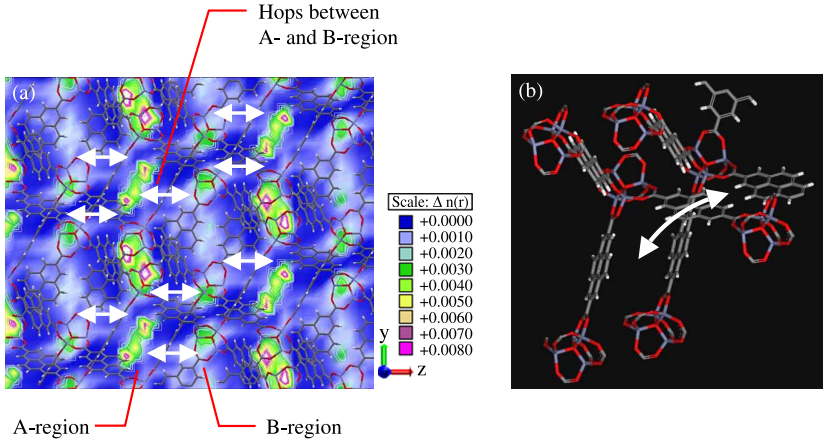

Figure 7. Contour plots of COM probability density of methane along the *z*-direction in IRMOF-13.

although the value of self-diffusion coefficient was affected largely, the diffusion mechanism remained unchanged for both flexible and rigid IRMOF-1.

4. Conclusion

This work shows that catenation can reduce diffusivity of methane by a factor of 3–5 at room temperature, which is much larger than that of hydrogen, attributed to the stronger interactions between methane and the frameworks of IRMOFs. A detail analysis of diffusion mechanism indicates that the molecule diffusion is mainly governed by the strong confinement in catenation regions, leading to a 3D diffusion via a jump sequence along the catenation regions in the catenated IRMOFs. Together, with the observations in our previous work [39], it is clear that both the adsorption selectivity and dynamic selectivity are enhanced for CH_4/H_2 mixtures in the catenated IRMOFs. Thus, catenation may be a good strategy to improve the overall performance of a material as a membrane in separation applications.

Acknowledgements

The financial support of the National Natural Science Foundation of China (nos. 20725622, 20821004 and 20876006) is greatly appreciated.

References

[1] G. Férey, *Hybrid porous solids: past, present, future*, Chem. Soc. Rev. 37 (2008), pp. 191–214.
[2] R.E. Morris and P.S. Wheatley, *Gas storage in nanoporous materials*, Angew. Chem. Int. Ed. 47 (2008), pp. 4966–4981.
[3] S. Horike, M. Dinca, K. Tamaki, and J.R. Long, *Size-selective lewis acid catalysis in a microporous metal–organic framework with exposed Mn^{2+} coordination sites*, J. Am. Chem. Soc. 130 (2008), pp. 5854–5855.
[4] B. Chen, X. Zhao, A. Putkham, K. Hong, E.B. Lobkovsky, E.J. Hurtado, A.J. Fletcher, and K.M. Thomas, *Surface interactions and quantum kinetic molecular sieving for H_2 and D_2 adsorption on a mixed metal–organic framework material*, J. Am. Chem. Soc. 130 (2008), pp. 6411–6423.
[5] B. Panella, K. Hönes, U. Müller, N. Trukhan, M. Schubert, H. Pütter, and M. Hirscher, *Desorption studies of hydrogen in metal–organic frameworks*, Angew. Chem. Int. Ed. 47 (2008), pp. 2138–2142.
[6] S. Ma, D. Sun, J.M. Simmons, C.D. Collier, D. Yuan, and H.C. Zhou, *Metal–organic framework from an anthracene derivative containing nanoscopic cages exhibiting high methane uptake*, J. Am. Chem. Soc. 130 (2008), pp. 1012–1016.
[7] H.J. Choi, M. Dincă, and J.R. Long, *Broadly hysteretic H_2 adsorption in the microporous metal–organic framework Co(1,4-benzenedipyrazolate)*, J. Am. Chem. Soc. 130 (2008), pp. 7848–7850.
[8] A.R. Millward and O.M. Yaghi, *Metal–organic frameworks with exceptionally high capacity for storage of carbon dioxide at room temperature*, J. Am. Chem. Soc. 127 (2005), pp. 17998–17999.
[9] R. Matsuda, R. Kitaura, S. Kitagawa, Y. Kubota, R.V. Belosludov, T.C. Kobayashi, H. Sakamoto, T. Chiba, M. Takata, Y. Kawazoe, et al., *Highly controlled acetylene accommodation in a metal–organic microporous material*, Nature 436 (2005), pp. 238–241.
[10] B. Xiao, P.S. Wheatley, X. Zhao, A.J. Fletcher, S. Fox, A.G. Rossi, I.L. Megson, S. Bordiga, L. Regli, K.M. Thomas, et al., *High-capacity hydrogen and nitric oxide adsorption and storage in a metal–organic framework*, J. Am. Chem. Soc. 129 (2007), pp. 1203–1209.
[11] L. Pan, D.H. Olson, L.R. Ciemnolonski, R. Heddy, and J. Li, *Separation of hydrocarbons with a microporous metal–organic framework*, Angew. Chem. Int. Ed. 45 (2006), pp. 616–619.
[12] M. Eddaoudi, J. Kim, N. Rosi, D. Vodak, J. Wachter, M. O'Keefe, and O.M. Yaghi, *Systematic design of pore size and functionality in isoreticular MOFs and their application in methane storage*, Science 295 (2002), pp. 469–472.
[13] S.S. Han, A.G. William III, *Lithium-doped metal–organic frameworks for reversible H_2 storage at ambient temperature*, J. Am. Chem. Soc. 129 (2007), pp. 8422–8423.
[14] K.S. Walton, A.R. Millward, D. Dubbeldam, H. Frost, J.J. Low, O.M. Yaghi, and R.Q. Snurr, *Understanding inflections and steps in carbon dioxide adsorption isotherms in metal–organic frameworks*, J. Am. Chem. Soc. 130 (2008), pp. 406–407.
[15] H. Frost and R.Q. Snurr, *Design requirements for metal–organic frameworks as hydrogen storage materials*, J. Phys. Chem. C 111 (2007), pp. 18794–18803.
[16] J.L. Belof, A.C. Stern, M. Eddaoudi, and B. Space, *On the mechanism of hydrogen storage in a metal–organic framework material*, J. Am. Chem. Soc. 129 (2007), pp. 15202–15210.
[17] N.A. Ramsahye, G. Maurin, S. Bourrelly, P. Llewellyn, T. Loiseau, and G. Ferey, *Charge distribution in metal organic framework materials: transferability to a preliminary molecular simulation study of the CO_2 adsorption in the MIL-53 (Al) system*, Phys. Chem. Chem. Phys. 9 (2007), pp. 1059–1063.
[18] N.A. Ramsahye, G. Maurin, S. Bourrelly, P. Llewellyn, C. Serre, T. Loiseau, T. Devic, and G. Ferey, *Probing the adsorption sites for CO_2 in metal organic frameworks materials MIL-53 (Al,Cr) and MIL-47 (V) by density functional theory*, J. Phys. Chem. C 112 (2008), pp. 514–520.
[19] T. Düren, L. Sarkisov, O.M. Yaghi, and R.Q. Snurr, *Design of new materials for methane storage*, Langmuir 20 (2004), pp. 2683–2689.
[20] Q. Yang, C. Zhong, and J. Chen, *Computational study of CO_2 storage in metal–organic frameworks*, J. Phys. Chem. C 112 (2008), pp. 1562–1569.
[21] T. Sagara, J. Klassen, and E. Ganz, *Computational study of hydrogen binding by metal–organic framework-5*, J. Chem. Phys. 121 (2004), pp. 12543–12547.
[22] G. Garberoglio, A.I. Skoulidas, and J.K. Johnson, *Adsorption of gases in metal organic materials: comparison of simulations and experiments*, J. Phys. Chem. B 109 (2005), pp. 13094–13103.
[23] F. Stallmach, S. Gröger, V. Künzel, J. Kärger, O.M. Yaghi, M. Hesse, and U. Müller, *NMR studies on the diffusion of hydrocarbons on the metal–organic framework material MOF-5*, Angew. Chem. Int. Ed. 45 (2006), pp. 2123–2126.
[24] P.V. Kortunov, L. Heinke, M. Arnold, Y. Nedellec, D.J. Jones, J. Caro, and J. Karger, *Intracrystalline Diffusivities and surface permeabilities deduced from transient concentration profiles: methanol in MOF manganese formate*, J. Am. Chem. Soc. 129 (2007), pp. 8041–8047.
[25] F. Salles, H. Jobic, G. Maurin, M.M. Koza, P.L. Llewellyn, T. Devic, C. Serre, and G. Ferey, *Experimental evidence supported by simulations of a very high H_2 diffusion in metal organic framework materials*, Phys. Rev. Lett. 100 (2008), pp. 245901–245904.
[26] A.I. Skoulidas, *Molecular dynamics simulations of gas diffusion in metal–organic frameworks: argon in CuBTC*, J. Am. Chem. Soc. 126 (2004), pp. 1356–1357.
[27] A.I. Skoulidas and D.S. Sholl, *Self-diffusion and transport diffusion of light gases in metal–organic framework materials assessed using molecular dynamics simulations*, J. Phys. Chem. B 109 (2005), pp. 15760–15768.
[28] Q. Yang and C. Zhong, *Molecular simulation of adsorption and diffusion of hydrogen in metal organic frameworks*, J. Phys. Chem. B 109 (2005), pp. 11862–11864.
[29] L. Sarkisov, T. Düren, and R.Q. Snurr, *Molecular modelling of adsorption in novel nanoporous metal-organic materials*, Mol. Phys. 102 (2004), pp. 211–221.
[30] Y.H. Jhon, M. Cho, H.R. Jeon, I. Park, R. Chang, J.L.C. Rowsell, and J. Kim, *Simulations of methane adsorption and diffusion within*

alkoxy-functionalized IRMOFs exhibiting severely disordered crystal structures, J. Phys. Chem. C 111 (2007), pp. 16618–16625.

[31] B. Liu, Q. Yang, C. Xue, C. Zhong, and B. Smit, *Molecular simulation of hydrogen diffusion in interpenetrated metal–organic frameworks*, Phys. Chem. Chem. Phys. 10 (2008), pp. 3244–3249.

[32] J. Liu, J.Y. Lee, L. Pan, R.T. Obermyer, S. Simizu, B. Zande, J. Li, S.G. Sankar, and J.K. Johnson, *Adsorption and diffusion of hydrogen in a new metal–organic framework Material: [Zn(bdc)(ted)$_{0.5}$]*, J. Phys. Chem. C 112 (2008), pp. 2911–2917.

[33] S. Keskin, J. Liu, J.K. Johnson, and D.S. Sholl, *Testing the accuracy of correlations for multicomponent mass transport of adsorbed gases in metal–organic frameworks: diffusion of H_2/CH_4 mixtures in CuBTC*, Langmuir 24 (2008), pp. 8254–8261.

[34] S. Keskin and D.S. Sholl, *Screening metal–organic framework materials for membrane-based methane/carbon dioxide separations*, J. Phys. Chem. C 111 (2007), pp. 14055–14059.

[35] S. Amirjalayer, M. Tafipolsky, and R. Schmid, *Molecular dynamics simulation of benzene diffusion in MOF-5: importance of lattice dynamics*, Angew. Chem. Int. Ed. 46 (2006), pp. 463–466.

[36] J.L.C. Rowsell and O.M. Yaghi, *Effects of functionalization, catenation, and variation of the metal oxide and organic linking units on the low-pressure hydrogen adsorption properties of metal–organic frameworks*, J. Am. Chem. Soc. 128 (2006), pp. 1304–1315.

[37] D.H. Jung, D. Kim, T.B. Lee, S.B. Choi, J.H. Yoon, J. Kim, K. Choi, and S.H. Choi, *Grand canonical Monte Carlo simulation study on the catenation effect on hydrogen adsorption onto the interpenetrating metal–organic frameworks*, J. Phys. Chem. B 110 (2006), pp. 22987–22990.

[38] S. Ma, D. Sun, M. Ambrogio, J.A. Fillinger, S. Parkin, and H.C. Zhou, *Framework-catenation isomerism in metal–organic frameworks and its impact on hydrogen uptake*, J. Am. Chem. Soc. 129 (2007), pp. 1858–1859.

[39] B. Liu, Q. Yang, C. Xue, C. Zhong, B. Chen, and B. Smit, *Enhanced adsorption selectivity of hydrogen/methane mixtures in metal–organic frameworks with interpenetration: a molecular simulation study*, J. Phys. Chem. C 112 (2008), pp. 9854–9860.

[40] B. Chen, C. Liang, J. Yang, D.S. Contreras, Y.L. Clancy, E.B. Lobkovsky, O.M. Yaghi, and S. Dai, *A microporous metal–organic framework for gas-chromatographic separation of alkanes*, Angew. Chem. Int. Ed. 45 (2006), pp. 1390–1393.

[41] L. Bastin, P.S. Bárcia, E.J. Hurtado, J.A.C. Silva, A.E. Rodrigues, and B. Chen, *A microporous metal–organic framework for separation of CO_2/N_2 and CO_2/CH_4 by fixed-bed adsorption*, J. Phys. Chem. C 112 (2008), pp. 1575–1581.

[42] S.J. Goodbody, K. Watanabe, D. MacGowan, J. Walton, and N. Quirke, *Molecular simulation of methane and butane in silicalite*, J. Chem. Soc, Faraday Trans. 87 (1991), pp. 1951–1958.

[43] A.K. Rappé, C.J. Casewit, W.A. Goddard III, and W.M. Skiff, *UFF, a full periodic table force field for molecular mechanics and molecular dynamics simulations*, J. Am. Chem. Soc. 114 (1992), pp. 10024–10035.

[44] R. Babarao, Z. Hu, and J. Jiang, *Storage and separation of CO_2 and CH_4 in silicalite, C_{168} schwarzite, and IRMOF-1: a comparative study from Monte Carlo simulation*, Langmuir 23 (2007), pp. 659–666.

[45] J. Jiang and S.I. Sandler, *Monte Carlo simulation for the adsorption and separation of linear and branched alkanes in IRMOF-1*, Langmuir 22 (2006), pp. 5702–5707.

[46] G. Martyna, M.E. Tuckerman, D.J. Tobias, and M.L. Klein, *Explicit reversible integrators for extended systems dynamics*, Mol. Phys. 87 (1996), pp. 1117–1157.

[47] O. Talu, M.S. Sun, and D.B. Shah, *Diffusivities of* n*-alkanes in silicalite by steady-state single-crystal membrane technique*, AIChE J. 44 (1998), pp. 681–694.

[48] T.C. Bowen, J.L. Falconer, R.D. Noble, A.I. Skoulidas, and D.S. Sholl, *A comparison of atomistic simulations and experimental measurements of light gas permeation through zeolite membranes*, Ind. Eng. Chem. Res. 41 (2002), pp. 1641–1650.